Performance analysis of brake discs in trains

Hiyam Adil Habeeb [1], Ahmed Esmael Mohan [1], Mohd Azman Abdullah [2*], Mohamad Hanif Abdul Aziz [2], Reduan Mat Dan [2], Mohd Hanif Harun [2]

[1] Al-Furat Al-Awsat Technical University, Technical College Al-Mussaib, 54003 Babylon, IRAQ.
[2] Fakulti Kejuruteraan Mekanikal, Universiti Teknikal Malaysia Melaka, Hang Tuah Jaya, 76100 Durian Tunggal, Melaka, MALAYSIA.
*Corresponding author: mohdazman@utem.edu.my

KEYWORDS	ABSTRACT
Brake disc Railway maintenance Commuter service Wear profile Wear	A complete analysis of the wear profiles of brake discs on commuter trains was carried out to evaluate their performance based on the rate of wear on the wheels. Actual data on the thickness and wear height of the discs were obtained at different mileages using a laser measurement device. The data were plotted to analyse the relationship between the wear and position of the brake discs at different axles. The wear rate of the discs was established to investigate the wear pattern. It was observed that the wear of the discs increased with decreasing thickness of the wear material and increasing wear height. The different positions of the discs also produced different wear profiles. The discs at the front and rear axles, experienced significant wear compared to the ones at the centre axle. The wear rate of the discs on the transit commuter rail (TCR) was higher than on the express commuter rail (ECR). This was due to the number of stops made on each trip, where the TCR stops at six stations unlike the ECR, which stops only at three stations. The higher the number of stops, the higher the frequency at which the brake discs have to be applied to stop the commuter train; thereby resulting in higher wear. Nevertheless, at certain locations along the tracks, usually where the tracks curve, the commuter trains are required to operate at a slow speed. This affects the amount of braking force that is applied to reduce the speed of the ECR as it operates at a high speed. The advantage for the TCR as it takes curves is that since the commuter train is already moving slowly, only a low braking force has to be applied, and thus, the wear on the brake disc is small.

1.0   INTRODUCTION

A disc brake system usually consists of a brake disc rotor, two brake pads and a calliper. The combination of these components enables a rotating wheel to experience severe braking in a short stopping distance (Hasegawa and Uchida, 1999). The brake disc, which is located on the axle of a wheel, has a circular aperture at its centre, and this is surrounded by a number of holes for the wheel bolts. The brake disc rotates along with the wheel. When the brakes are actuated, a normal load is produced, resulting in the generation of an in-plane friction force at the disc-pad interface (Sano et al., 2015). This, in turn, produces a brake torque at the centre of rotation of the wheels. The reaction to the brake torque is represented as the braking force, which slows the vehicle.

The brake disc works when stress is exerted by the two brake pads on opposite sides of the rotor. The brake pads are installed inside the calliper that is located above the rotating disc. All the components of the brake disc system are open to air circulation, which allows for cooling of the brake elements. Disc brakes are extensively used to reduce speed through friction of the material.

Brake discs are commonly made of a material called grey cast iron due to its superior heat handling and damping (vibration absorption) characteristic (Goo and Lim, 2015). The specifications for the manufacture of grey iron for various applications are maintained by the SAE (Society of Automotive Engineers). These specifications determine the best range of hardness, chemical composition, tensile strength, and other properties required for the intended use. Brake discs are made of different materials, depending on the type of application (Talib et al., 2018).

Commuter trains also make use of disc brake systems. In order to bring the wheels to a stop, the brake pads, which are made of friction materials, are mechanically, hydraulically, pneumatically, or electromagnetically forced against both sides of the brake disc to cause the wheels to slow down and stop. When a braking force is applied, the brake discs will become hot. Moreover, if a braking force is frequently applied, heat will be maintained in the brake discs and brake pads, and there will be no time for cooling (Hasegawa and Uchida, 1999). The discs are usually made of cast steel, grey cast iron or aluminium. Both the brake discs and brake pads are subject to wear. The wear rates tend to be high, and braking may be poor or grabby when the brake disc is hot (Yevtushenko, 2019; Kim et al., 2008; and Panier et al., 2004). The wear mechanisms in braking systems have been studied by several researchers over the years (Abbasi et al., 2011; Wang et al., 2017; Futáš et al., 2019; Wu et al., 2016; Sakamoto and Hirakawa 2005; and Yang and Yang, 2018), including the noise generated by brake systems (Wang et al., 2019 and Chen et al., 2019). These are quite unpredictable due to the contact variations that exist in these specific and complex systems. Uniform wear on brake discs and brake pads cannot be achieved due to various braking forces and brake pressure distributions. The unequal pressure distribution causes uneven wear, thereby shortening the life of the brake disc (Sharma et al., 2015). This might lead to more frequent tapered wear disc replacements. The dynamic contact pressure distribution in a disc brake system remains impossible to measure through experimental methods. Braking force is generated by way of friction between the disc pads when they are squeezed in opposition to the disc rotor (Sano et al., 2015). Since brake discs, unlike brake drums, do not use friction between the liner and rotor to increase the braking strength, they are less likely to result in a pull. The friction surface is constantly exposed to the air, ensuring true dissipation of heat, thereby minimizing brake wear. In addition, it enables self-cleaning as dust and water are thrown off, thus lowering the difference in friction.

The commuter train is a passenger rail transport service that primarily operates between city centres. In this paper, the commuter rail system connecting the Kuala Lumpur International

Airport to Kuala Lumpur Sentral was studied. This rail system is comprised of two types of commuter trains, namely, express and transit. The distance between the two places is 59 kilometres (Figure 1) (Abdullah et al., 2014 and Abdullah et al., 2018).
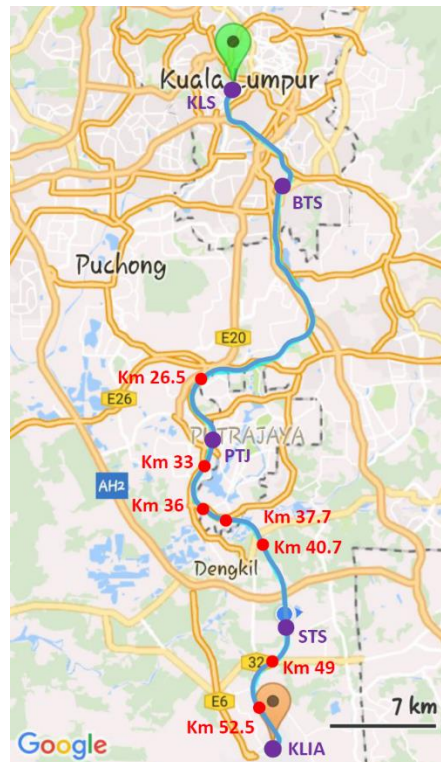

Figure 1: Commuter track route (Abdullah et al., 2014; Abdullah et al., 2018).

Trains that operate at high velocities require braking structures that produce better braking forces, thereby resulting in a more rapid depletion of larger amounts of electrical power, not to mention the problem of wear inside the brake casings (Sawczuk and Tomaszewski, 2013). The distances travelled by commuter trains are specifically observed when it comes to the installation of disc brakes on the wheels. Previously, due to curved tracks, only dynamic vibrations and swaying were observed during the operation of commuter trains (Abdullah et al., 2018). The slowing down of a commuter train is observed by the reduction in its longitudinal acceleration (Abdullah et al., 2014).

In this paper, a complete data analysis on the wear profiles of the brake discs on commuter trains was carried out to effectively evaluate the performance of the brake discs, and to determine a suitable maintenance schedule based the brake disc wear profile trend. Data on the wear profiles of the brake discs of the express commuter rail (ECR) and transit commuter rail (TCR) were recorded and analysed.

2.0 EXPERIMENTAL PROCEDURE

The axle orientations of the commuter train are shown in Figure 2. Axle no. 1 is located and began at side A (driver cab A) of the commuter train. The brake discs are mounted on 8 axles, while axle's no. 5 and 6 are trailing axles with no brake system. Each axle consists of two wheels, and each wheel is mounted with 2 brake discs, an inner and outer brake disc. The brake discs are identified by numbers, for example, 1RI denotes the inner brake disc on the right side of axle number one, and 1RO denotes the outer brake disc on the right side of axle number one. Figure 3 shows the thickness and height for the wear profile of a brake disc. The wear profile of the brake disc is important in order to analyse the wear condition of the brake disc. The thickness, T, of the wear material on the brake disc, and the height, H, of the wear hole are measured in millimetres (mm) at different distances in kilometres (km).
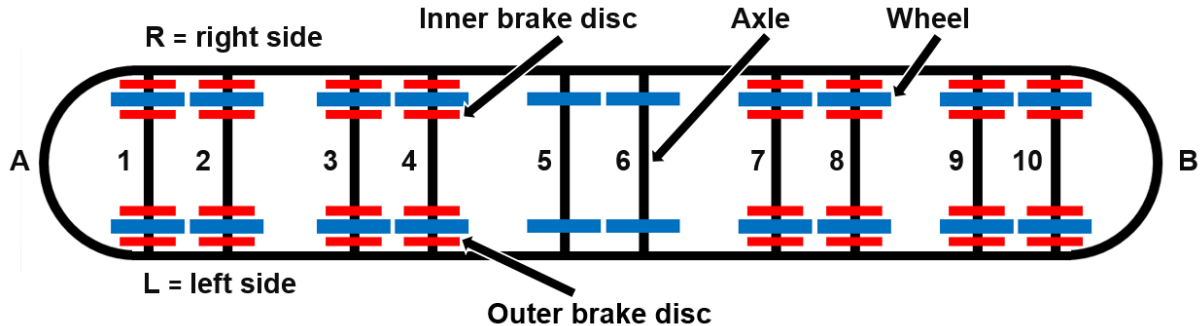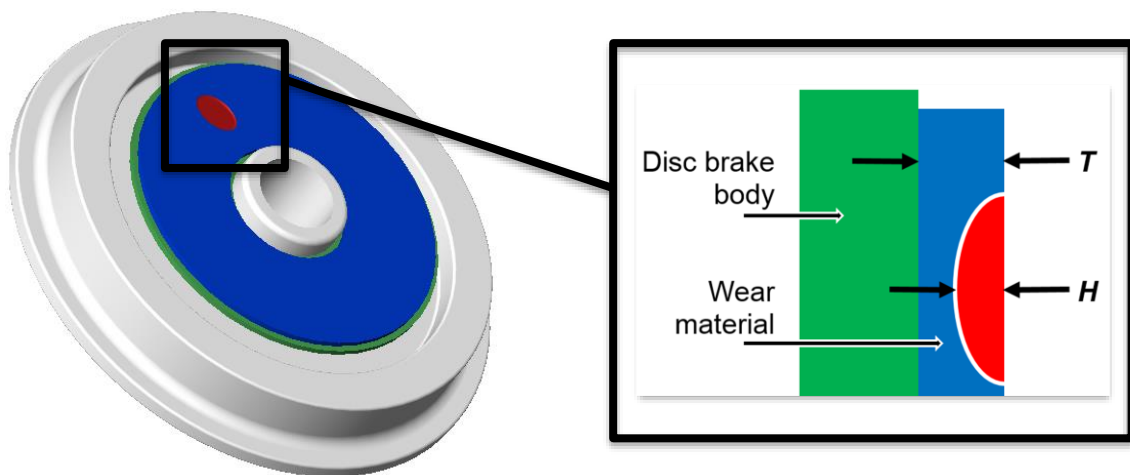

Figure 2: Orientation of brake discs.

Figure 3: Wear profiles of brake discs.

A Calipri laser is used to measure the wear profiles of brake discs. It applies measurement standards of JCGM100:2008, DIN V ENV 13005:1999-06, DIN EN 13715:2001-01, DIN EN 15313:2016-09, DIN 27201-9:2017-06 (NextSense, 2020). It involves an innovative technology that automatically corrects the tilts and rotations of the measurement device. Due to laser light section technology, the compact measurement device can be aligned with the brake disc without

mechanical mounting. A sensor records the complete wear profile, and clearly shows both the actual and target values on the display and on a tablet or personal computer using Calipri software. Figure 4 shows the procedure for measuring the wear profile of a brake disc using the Calipri laser equipment. According to the manual for the equipment, the repeatability value is +/- 35 μm, the standard deviation for all the measuring points is +/- 15 μm, and the absolute uncertainty value is +/- 80 μm (NextSense, 2020).

Figure 4: Measurement of brake disc wear profile using Calipri laser.

3.0   RESULTS AND DISCUSSION

Table 1 shows the measurement data of the brake discs for the transit commuter rail (TCR), while Table 2 presents the data for the express commuter rail (ECR). The initial mileage of the TCR was 5587839 km, and that of the ECR was 6181961 km.

Figure 5 shows the average wear height, H for each axle of the ECR and TCR. It was observed that the TCR had a higher wear compared to the ECR. Since the TCR had to stop at a total of 6 stations compared to the ECR, which had to stop at only 3 stations, the number of braking operations was high for the TCR. Due to the frequent braking, the wear on the brake discs was high for the TCR. With regard to T, the average thickness of the wear material, the data for the ECR was higher than for the TCR (Figure 6).

Table 1: Brake disc data for TCR.

| Disc | Mileage (km) | | | | | |
| | 5587839 | | 5619449 | | 5645345 | |
	H (mm)	T (mm)	H	T	H	T
1LI	0.98	4.76	1.01	5.06	1.16	4.85
1LO	1.03	4.85	1.38	4.9	1.12	4.87
1RI	0.96	4.85	0.98	4.24	1.31	4.94
1RO	0.92	4.75	1.07	4.88	1.05	4.87
2LI	1.04	4.90	1.13	4.87	1.33	4.95
2LO	1.00	4.89	1.14	4.93	1.38	4.88
2RI	1.20	4.89	1.32	4.81	1.07	4.79
2RO	1.15	4.99	1.07	4.88	1.31	4.89
3LI	0.96	4.88	1.11	4.90	1.23	4.88
3LO	1.09	4.87	1.13	4.83	1.31	4.95
3RI	1.05	4.91	1.19	4.88	1.41	4.95
3RO	1.14	4.98	1.45	4.90	1.46	4.95
4LI	1.18	4.73	1.10	4.75	1.40	5.05
4LO	1.13	4.80	1.54	5.01	1.57	5.05
4RI	0.96	4.66	1.14	4.73	1.27	4.74
4RO	1.14	4.62	1.34	5.05	1.37	4.89
7LI	0.89	4.93	1.06	4.91	1.25	4.87
7LO	1.13	4.99	1.04	4.85	1.02	4.94
7RI	0.84	4.89	1.00	4.92	1.20	4.96
7RO	1.01	4.87	1.25	4.93	1.32	4.93
8LI	1.08	4.83	1.21	4.96	1.49	4.94
8LO	1.23	4.84	1.44	4.99	1.36	4.97
8RI	1.19	4.86	1.16	4.88	1.29	4.89
8RO	1.07	4.89	1.35	4.99	1.33	5.07
9LI	1.14	4.97	1.38	4.87	1.39	4.97
9LO	1.37	5.06	1.73	4.87	1.60	5.00
9RI	1.50	4.64	1.82	4.15	1.91	4.84
9RO	1.50	4.79	1.72	4.76	1.89	5.05
10LI	1.42	4.82	1.48	4.41	1.75	4.86
10LO	1.32	4.78	1.63	4.85	1.77	4.81
10RI	1.41	4.80	1.61	4.85	1.68	4.88
10RO	1.38	4.94	1.57	4.95	1.60	4.92

Table 2: Brake disc data for ECR.

Disc	Mileage (km)					
	6181961		6274660		6423697	
	H (mm)	T (mm)	H	T	H	T
1LI	0.24	4.83	0.41	4.83	0.63	4.64
1LO	0.31	4.94	0.34	4.79	0.57	4.64
1RI	0.18	4.91	0.27	4.94	0.63	4.72
1RO	0.15	4.98	0.43	4.91	0.39	4.83
2LI	0.37	4.19	0.32	4.84	0.74	4.37
2LO	0.21	4.94	0.51	4.91	0.47	2.24
2RI	0.36	4.75	0.28	4.81	0.68	4.46
2RO	0.36	4.96	0.43	4.91	0.46	4.79
3LI	0.22	4.91	0.46	4.92	0.54	4.80
3LO	0.25	4.94	0.42	4.91	0.63	2.37
3RI	0.13	4.80	0.22	4.90	0.44	4.79
3RO	0.36	4.93	0.58	4.90	0.43	4.78
4LI	0.36	4.58	0.31	4.75	0.51	4.81
4LO	0.18	4.95	0.46	4.90	0.73	1.86
4RI	0.24	4.82	0.28	4.87	0.61	5.00
4RO	0.21	4.87	0.35	4.97	0.59	4.76
7LI	0.14	4.91	0.31	4.91	0.56	4.89
7LO	0.26	4.92	0.40	5.00	0.57	4.37
7RI	0.14	4.95	0.29	4.89	0.56	4.83
7RO	0.26	4.93	0.38	4.92	0.41	4.87
8LI	0.12	4.81	0.36	4.76	0.43	4.84
8LO	0.33	5.01	0.48	4.98	0.67	2.68
8RI	0.33	4.42	0.35	4.85	0.58	4.86
8RO	0.32	4.76	0.55	4.93	0.67	4.46
9LI	0.24	5.00	0.32	4.95	0.53	4.75
9LO	0.17	4.94	0.39	4.87	0.51	3.98
9RI	0.20	4.99	0.39	4.94	0.53	4.89
9RO	0.32	4.97	0.29	5.00	0.71	4.35
10LI	0.24	4.24	0.50	4.74	0.46	4.67
10LO	0.14	4.95	0.53	4.88	0.55	2.60
10RI	0.14	4.57	0.22	4.88	0.59	4.79
10RO	0.30	4.91	0.44	4.91	0.55	3.70

It was assumed that during long-distance braking intervals between stations, a more uniform braking force was applied compared to short-distance braking intervals. Therefore, the brake mechanism caused the wear on the brake discs and brake pads to be evenly distributed. This happened to the brake discs on the ECR. The steady wear due to the braking activities reduced the thickness of the brake disc material instead of creating a hole in the disc itself. It can be seen in Figure 6 that the value of T for axle 1 was higher for the TCR than for the ECR. This went against the trend for the other axles. This was perhaps due to technical issues with regard to the braking mechanism for axle 1 in the ECR, where it produced such a high braking force on the brake discs that a slightly higher value of wear material thickness was obtained.

Figures 7 and 8 show the wear rate per 10^6 km of mileage (mm/1M km) of the discs for their respective H and T values. It can be observed that the TCR had a higher wear rate than the ECR. Nevertheless, based on the manual for the commuter train, the replacement of the brake disc is performed when the wear height, H is more than 1 mm. In this case, the average wear rates for H were 47.4 mm/1M km and 1.31 mm/ 1M km for the TCR and ECR, respectively. Therefore, the average mileage values for the brake disc replacement were 21097 km and 7633587 km for the TCR and ECR, respectively. This was true according to the data shown in Table 1 and Table 2. In Table 1, assuming 5587839 kilometres was the initial mileage, and the second reading was taken at 5619449 kilometres, hence, the difference in the mileage was about 31610 km. Within this mileage, the value of H for 1LI was 1.01 mm. According to the manual, when the value of H is more than 1 mm, the brake disc must be replaced. In Table 2, assuming 6181961 kilometres was the initial mileage, and the second reading was taken at 6274660 km, then, the difference in the mileage was about 92699 km. The value of H for 1LI was 0.41 mm. Therefore, the brake disc could still be used for the commuter operations.
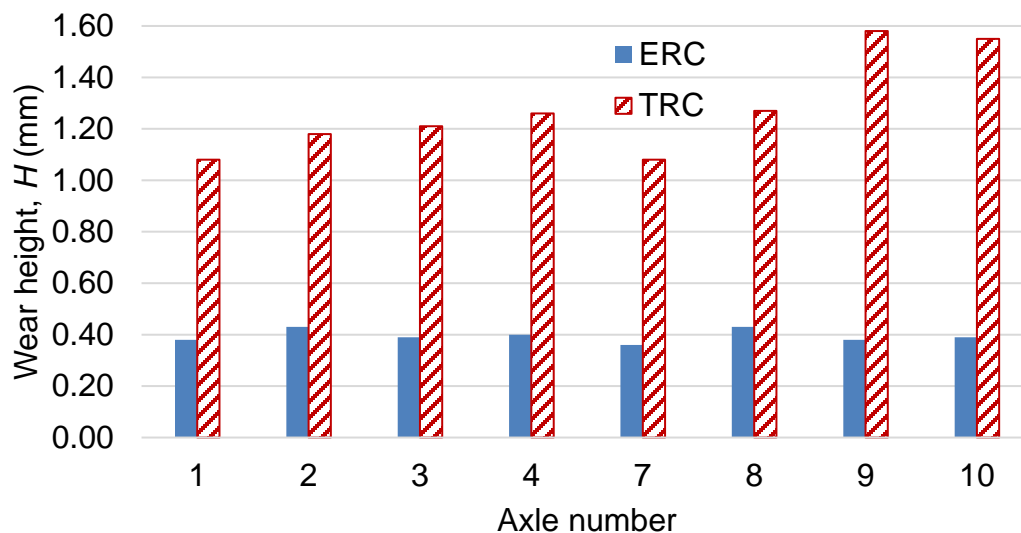

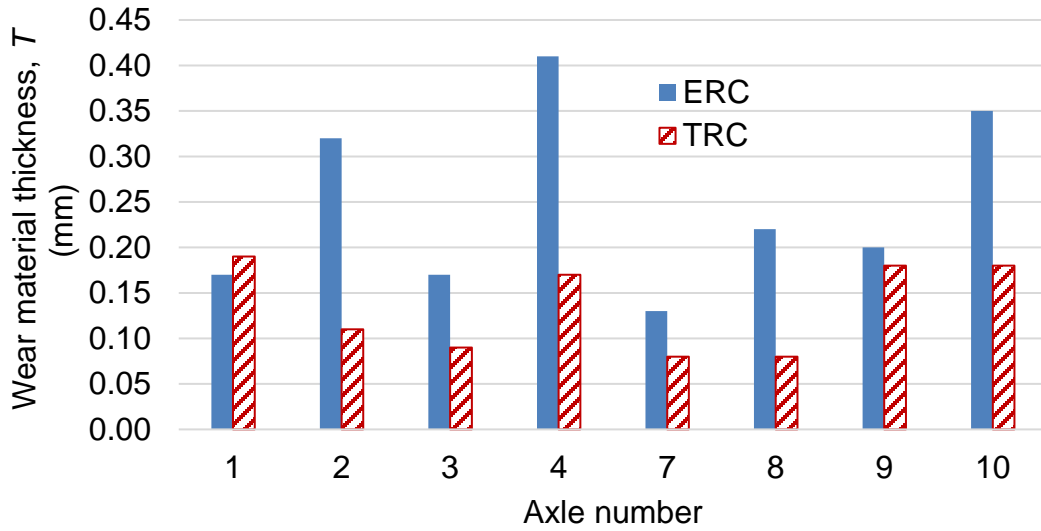Figure 5: Average total wear height of brake discs for each axle.

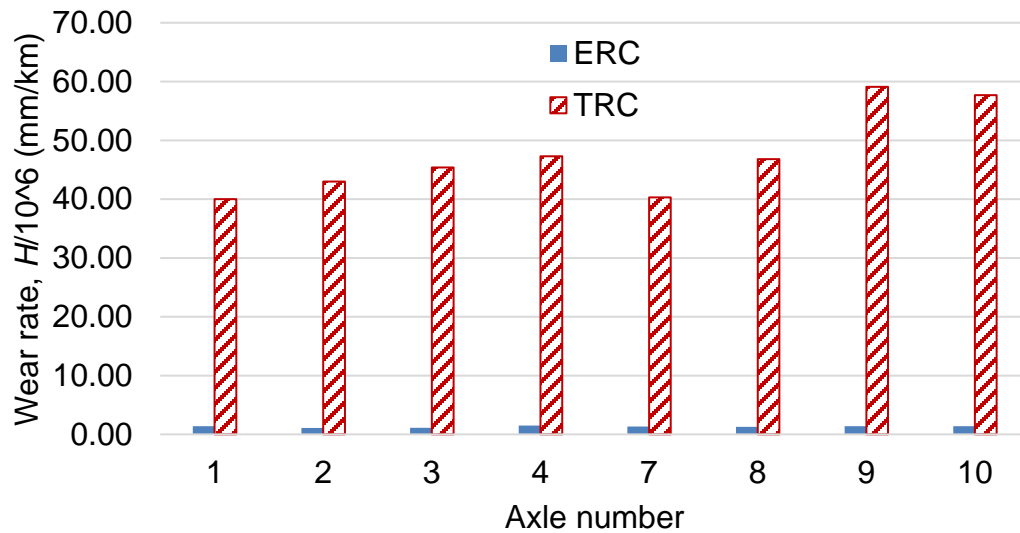Figure 6: Average total wear material thickness of brake discs for each axle.

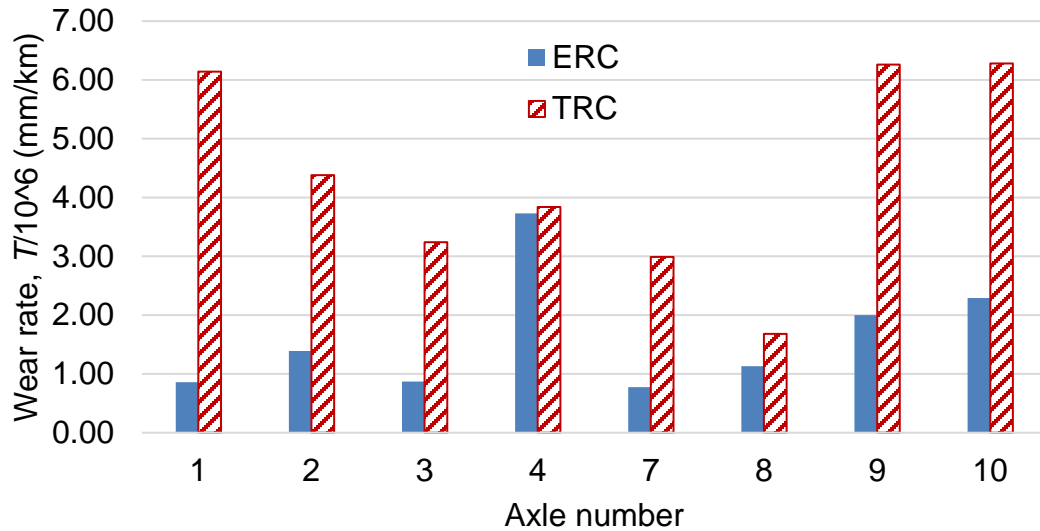Figure 7: Average total wear rate (mm/km) for H of brake discs for each axle.

Figure 8: Average total wear rate (mm/km) for T of brake discs for each axle.

Figures 9 and 10 show comparisons of the average wear for the inner and outer brake discs. It was observed that for the wear thickness, T, the wear on the outer disc was higher than on the inner disc for both the ECR and TCR. The calliper holds the brake pads on both sides of the wheel. Assuming the braking activity is consistent, the different wear values between the inner and outer discs describe the difference in the applied braking force. Due to the braking moment on the brake calliper, the calliper tends to bend inward. This produces a low contact force on the inner disc but a high contact force on the outer disc.

Figures 11 and 12 compare the average wear of the left and right brake discs for the ECR and TCR. The left brake disc had a higher wear compared to the right brake disc for both the ECR and TCR. Since the orientation of the train is fixed (Abdullah et al. 2014 and Abdullah et al. 2018), the left and right sides of the train are always fixed (Figure 1). Therefore, the accumulated lateral displacement of the train results in a difference in the force that is applied to stop the train. Thus, this was the reason for the difference in wear on the discs. Since the left disc experienced a higher wear, perhaps more passengers were loaded onto the left side of the train. This made the contact force on the left brake disc higher compared to the right brake disc. The high contact force due to the high vertical load increased the wear.
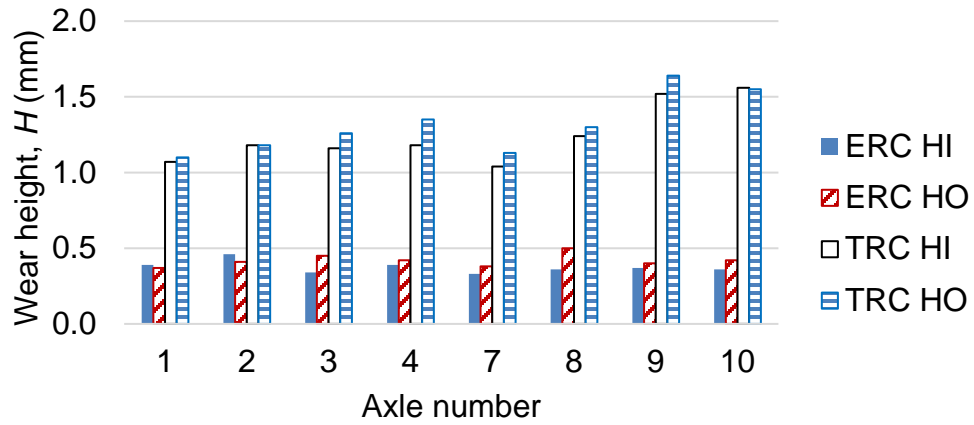
Figure 9: Comparison of the average total wear thickness of the material of the inner and outer brake discs of each axle.
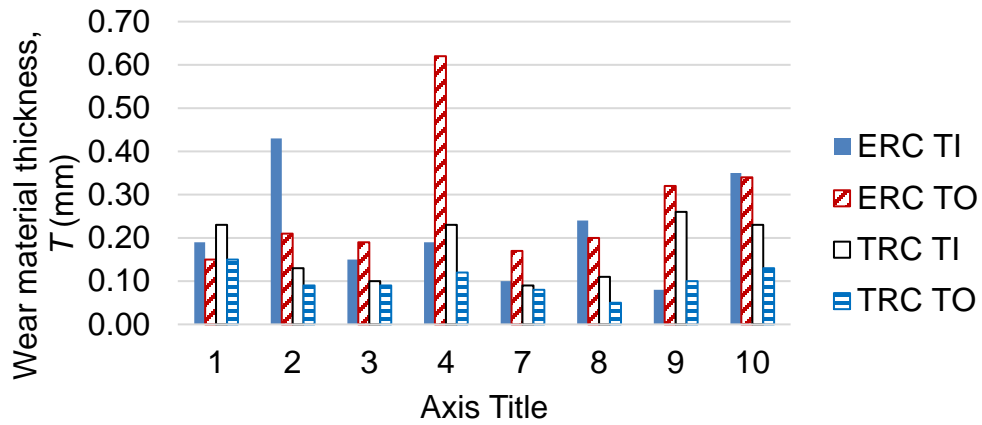

Figure 10: Comparison of average total wear thickness of the material of inner and outer brake discs of each axle.
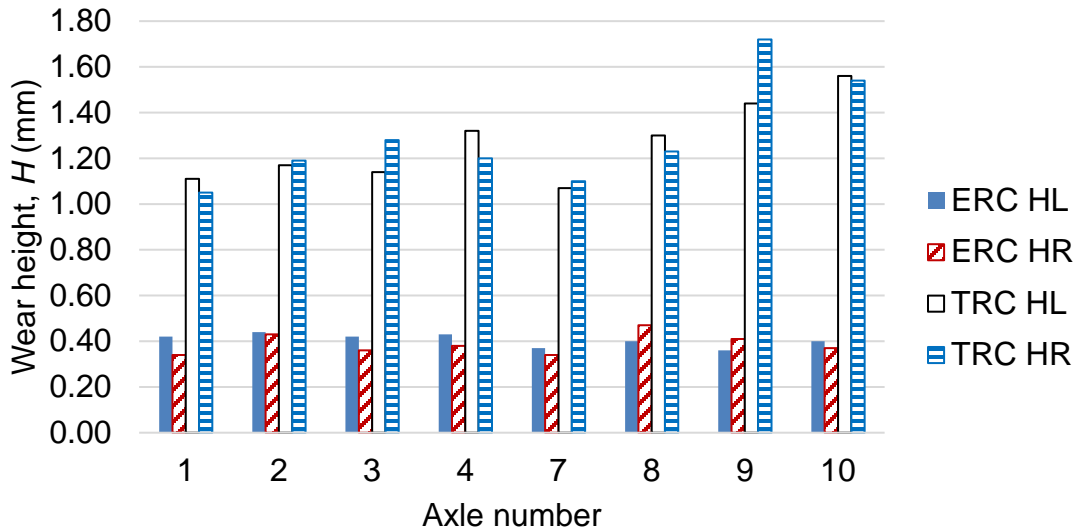
Figure 11: Comparison of average total wear thickness of the material of the left and right brake discs of each axle.
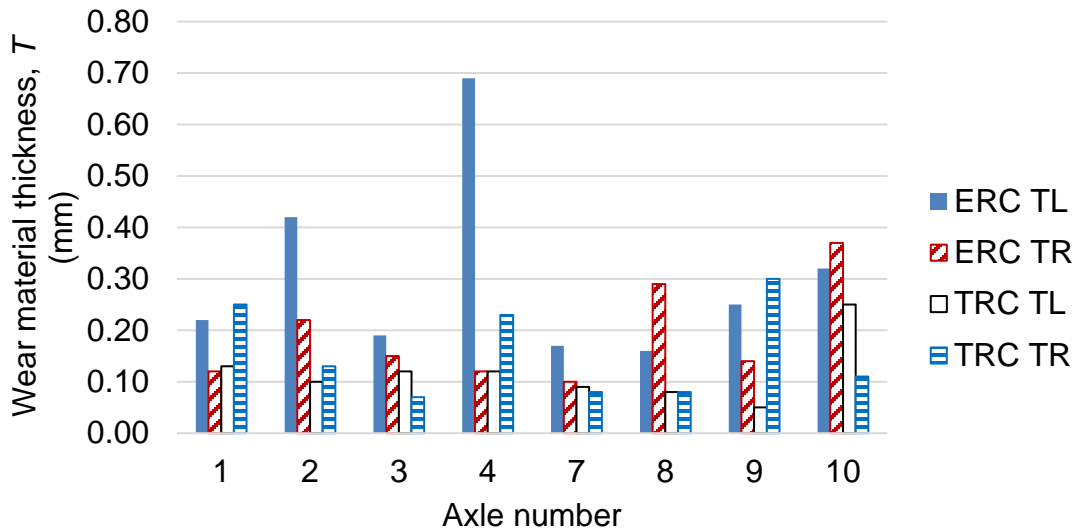

Figure 12: Comparison of average total wear thickness of the material of left and right brake discs of each axle.

Table 3 shows the average values of H and T for both the ECR and TCR. In the table, the TCR had an average H value of 1.28 mm, which was higher than that of the ECR (0.40 mm). However, the average T value of the TCR was 0.14 mm, which was smaller than that of the ECR (0.25 mm). This was due to the uniform braking by the ECR, without frequent braking and stopping. The uniform braking of the ECR affected only the wear thickness of the material. The braking force

was distributed equally throughout the discs. The frequent braking of the TCR affected the wear thickness of the brake discs. Many wear holes were visible on the discs, and these would reduce the reliability and life of the discs. The discs may fail or maintenance must be performed. The wear rate of the discs correspondingly supported the significant wear phenomenon on the TCR compared to the ECR. The value of the wear rate of H for the TCR was 47.45 mm per million km compared to the ECR, which was only 1.31 mm per million km. The values of H and T in relation to the inner and outer discs on the same wheel were more or less about the same since the wear effect was produced by the same brake calliper generating the same braking force. On comparing the average values of H and T for the left and right sides of the train, it was observed that for the ECR, the H and T wear values on the left side were greater than on the right side. This was due to the condition of the railway tracks. Since the train was operating in the same position, the driver cabs, A and B (Figure 1), were fixed facing the KLIA station and KLS station, respectively (Figure 1), there was no dismantling of the train body, and the train experienced the same rolling and yawing effects (Abdullah et al. 2014 and Abdullah et al. 2018). According to the track route (Figure 1), there were many curves, with the outer radius being higher than the inner radius when turning to the right. Therefore, the train experienced high roll and yaw moments on the left side. Due to these conditions, the braking effort was high for the brake disc on the left side compared to the right side of the train. In contrast, for the TCR, the wear on the right side was higher than on the left because most of the passengers sat or stood on the right side of the train. At the extra 3 stations where the TCR stopped, the doors of the train opened on the right side for disembarkation. Therefore, the passengers tended to sit or stand on the right side of the train for easy disembarkation. The heavier passenger load on the right side of the train caused a higher braking force to be applied on the discs.

Table 3: Average values.

Parameter	Average value		Unit
	ECR	TCR	
H	0.40	1.28	mm
T	0.25	0.14	mm
Wear rate H	1.31	47.45	mm/ 10^6 km
Wear rate T	1.63	4.35	mm/ 10^6 km
H on inner disc	0.37	1.24	mm
H on outer disc	0.42	1.31	mm
T on inner disc	0.22	0.17	mm
T on outer disc	0.27	0.10	mm
H on left side	0.40	1.26	mm
H on right side	0.39	1.29	mm
T on left side	0.30	0.12	mm
T on right side	0.19	0.16	mm

4.0   CONCLUSION

It could be concluded from the results that the wear rate of the brake discs of the TCR was higher than on those of the ECR. This was mainly due to the number stops that the trains had to make at the stations. The TCR stopped at a total of 6 stations between Kuala Lumpur Sentral (KLS) station and KLIA2. However, the ECR only stopped at KLIA between KLS and KLIA2. The higher the number of stops, the higher the braking frequency; thereby increasing the accumulative wear on the brake discs. However, this is true assuming the frequency of operations for both the TCR and ECR is the same on a daily basis. Due to the high wear and wear rate, the maintenance cost for the TCR is thus higher than for the ECR. The life of the ECR brake discs is at least 3 times higher than that of the ECR brake discs. Using this data and analysis, the frequency of maintenance processes as well as the predicted maintenance can be prepared based on the trend of the wear profiles. The operators of the ECR and TCR may use the data analysis to their advantage in the maintenance and planning of their operations. Such results and wear trends are also useful for maintenance strategies, and are applicable for the same model of trains operating elsewhere.

REFERENCES

Abbasi, S., Wahlström, J., Olander, L., Larsson, C., Olofsson, U., & Sellgren, U. (2011). A study of airborne wear particles generated from organic railway brake pads and brake discs. Wear, 273(1), 93-99.

Abdullah, M. A., Ramli, F. R., & Lim, C. S. (2014). Railway Dynamics Analysis Using Lego Mindstorms. In Applied Mechanics and Materials (Vol. 465, pp. 13-17). Trans Tech Publications Ltd.

Abdullah, M. A., Hassan, N. A., Foat, N. A. M., Shukri, M. F. A. M., & Mohan, A. E. (2018). Swaying Phenomenon of Express Railway Train in Malaysia, Proceedings of Innovative Research and Industrial Dialogue'18, July 2018, pp. 98-99.

Chen, G. X., Lv, J. Z., Zhu, Q., He, Y., & Xiao, X. B. (2019). Effect of the braking pressure variation on disc brake squeal of a railway vehicle: Test measurement and finite element analysis. Wear, 426, 1788-1796.

Futáš, P., Pribulová, A., Fedorko, G., Molnár, V., Junáková, A., & Laskovský, V. (2019). Failure analysis of a railway brake disc with the use of casting process simulation. Engineering Failure Analysis, 95, 226-238.

Goo, B. C., & Lim, C. H. (2010). Thermal fatigue evaluation of cast iron discs for railway vehicles. Procedia Engineering, 2(1), 679-685.

Hasegawa, I., & Uchida, S. (1999). Braking systems. Japan Railway and Transport Review, 20, 52-59.

Kim, J. G., Goo, B. C., Yoon, S. C., & Kwon, S. T. (2008). Thermographic investigation of hot spots in railway brake discs. In Key Engineering Materials (Vol. 385, pp. 669-672). Trans Tech Publications Ltd.

NextSense (2020). An ode to Calipri C40. Link: https://www.nextsense-worldwide.com/en/an-ode-to-calipri-c40.html, Last accessed 20/05/2020.

Panier, S., Dufrénoy, P., & Weichert, D. (2004). An experimental investigation of hot spots in railway disc brakes. Wear, 256(7-8), 764-773.

Sakamoto, H., & Hirakawa, K. (2005). Fracture analysis and material improvement of brake discs. JSME International Journal Series A Solid Mechanics and Material Engineering, 48(4), 458-464.

Sano, T., Endo, Y., Nakazawa, S. I., & Hijikata, D. (2015). On estimation of tangential force in railways brake systems by fuzzy inference. Journal of Advanced Computational Intelligence and Intelligent Informatics, 19(5), 639-644.

Sawczuk, W., & Tomaszewski, F. (2013). Evaluation of the wear of friction pads railway disc brake using selected frequency characteristic of vibrations signal generated by the disc brake. Diagnostyka, 14(3), 69-74.

Sharma, R. C., Dhingra, M., & Pathak, R. K. (2015). Braking systems in railway vehicles. International Journal of Engineering Research & Technology, 4(1), 206-211.

Talib, R. J., Selamat, M. A., Nordin, N. A., Jumahat, A., Sharudin, H., Zaharudin, A. M., & Pinang, C. P. (2018). Aptness of Kenaf powder as a friction modifier in the fabrication of brake friction material by powder metallurgy route. Jurnal Tribologi, 19, 121-131.

Wang, D. W., Mo, J. L., Liu, M. Q., Li, J. X., Ouyang, H., Zhu, M. H., & Zhou, Z. R. (2017). Improving tribological behaviours and noise performance of railway disc brake by grooved surface texturing. Wear, 376, 1586-1600.

Wang, Z., Han, J., Domblesky, J. P., Li, Z., Fan, X., & Liu, X. (2019). Crack propagation and microstructural transformation on the friction surface of a high-speed railway brake disc. Wear, 428, 45-54.

Wu, S. C., Zhang, S. Q., & Xu, Z. W. (2016). Thermal crack growth-based fatigue life prediction due to braking for a high-speed railway brake disc. International Journal of Fatigue, 87, 359-369.

Yang, G., & Yang, Y. (2018). Investigation on the thermal fatigue life evaluation method of railway brake disc with new material. Tehnički vjesnik, 25(4), 1095-1102.

Yevtushenko, A., Kuciej, M., & Wasilewski, P. (2019). Experimental study on the temperature evolution in the railway brake disc. Theoretical and Applied Mechanics Letters, 9(5), 308-311.